Introduction

The seismic methods have the highest resolution among surface geophysical technologies, and utilise many reliable imaging techniques. At the present time, reflection seismic technologies play an important role for oil and gas exploration and play the leading role in identifying the hydrocarbon deposits in sedimentary basins. These methods are utilised to build 3D geological models of oil and gas deposits and to monitor production processes. Despite of the successful applications of surface seismic in sedimentary environments, these methods are not so widespread in the mining industry. One of the reasons is the high cost of seismic surveys in comparison with conventional (electromagnetic and potential) geophysical methods. Another is that seismic methods are difficult to apply in hard rock environments because of the complex and inhomogeneous structure of this media.

Hard rock sites consist of igneous and metamorphic rocks and often have rather sophisticated geological structure, which includes a lot of faults, fracture zones, steep dips, etc. Such environments are also often characterized by difficult topographic and near-surface situations. These circumstances could lead to different and unstable conditions for generating and recording of seismic waves, and as a result, the field data could have an anomalously low signal-to-noise ratio that may affect the final subsurface image. In general, hard rock media have high propagation velocities of elastic waves, which translates to long wavelengths; this can also affect seismic resolving power, because often the seismic acquisitions are carried out with an insufficient frequency range. In such conditions, some conventional seismic migration algorithms have difficulties in constructing reliable images of targets.

Most of the seismic migrations need a velocity model of geological section. In sedimentary environments, where boundaries between the layers are usually horizontal and continuous reflectors, velocities could be calculated directly from seismic data. However, in hard rock conditions, there are many steep dips and sustained boundaries are lacking. That is why the estimation of velocities becomes a nontrivial problem. In addition, there are not enough acoustic logs performed during the mining exploration, which provide important information about the wave propagation velocities. For these situations when there is not suitable velocity model available, imaging methods that do not require velocity model seem to be the most suitable. Herein, we describe an application of such a velocity-less imaging algorithm to synthetic models. One of the models is based on a real hard rock geological situation. This presented algorithm is based on estimation of horizontal slownesses (local event slopes) that are used to produce the migration attributes (the location of the migrated event as well as the migration velocity).

Description of migration algorithm

The first concepts of evaluation local slopes from pre-stack data and using them to estimate migration velocities and locations go back to Rieber (1936) and Riabinkin (1957). The idea of the velocity independent imaging method for migration of horizontal reflectors was suggested in paper by Ottolini (1983b); he presented the principle of building the image by applying the time dips of the seismic data at every point on the registered data. Fomel (2007) expanded the Ottolini's concept; he used information about local event slopes from common-midpoint and common-offset domains to get the complete data about the reflection geometry. Cooke et al. (2009) reported about using horizontal slownesses (local event slopes) to perform time imaging, estimation of velocities, and suppression of multiplies; these approaches were needed horizontal slownesses in common-shot and common-receiver domains. Bóna (2009) suggested the velocity-less pre-stack migration method, where only one (common-shot or common-receiver) domain is required to estimate the local event slopes.

Here we use the velocity-independent time migration, which based on computation of the horizontal slownesses for common-shot and common-receiver gathers and obtaining the values of parameters: migration velocity (V), vertical traveltime (t_0) and horizontal coordinates of the migrated reflection point (x_m). The expressions for these attributes were derived for 2D case by Cooke et al. (2009) from the double-square-root equation.

$$x_m = x_s - (x_r - x_s)p_s \frac{t-(x_r-x_s)p_r}{t(p_r-p_s)+2(x_r-x_s)p_s p_r} \quad (1)$$

$$V^2 = \frac{x_s-x_m}{tp_s} + \frac{x_r-x_m}{tp_r} \quad (2)$$

$$t_0 = \frac{|x_s-x_m|}{V}\frac{\sqrt{\frac{1}{V^2}-p_s^2}}{|p_s|} \quad (3)$$

These equations are obtained using the partial derivatives of double-square-root equation with respect to a shot and receiver gather directions. The equations 1 – 3 represent a system with three unknown migration parameters. Here, p_r and p_s are values of local event slopes measured in common-shot and common-receiver gathers respectively; x_s and x_r are the locations of source and receiver; t is the traveltime. For all points in the time domain the traveltime and coordinates of shots and receivers are known, values of p_r and p_s could be derived from seismic data as well. The final image is constructed by replacing each value of the input amplitudes to corresponding output location according to calculated t_0 and x_m attributes. Eventually, the obtained migration velocities can be used for suppression of multiples (Cooke et al., 2009) or as a starting velocity model in the standard imaging process.

Several techniques could be used to estimate the local event slopes for any point in the seismic dataset. The well-known conventional method for this aim is the local slant stack (Ottolini, 1983a). Another algorithm measures local event slopes by applying so-called plane-wave destruction filters (Fomel, 2002). The approach for estimation horizontal slownesses using the correction to linear plane-wave destructors was suggested by Schleicher et al. (2009). This corrected estimator produces good results even if there is a high noise level in the data. Here we used a method based on semblance to derive the values of the local event slopes. For a specified range of slownesses, using parabolic interpolation, we shifted traces in chosen neighbourhoods for each value of local slopes and calculated the semblance in a running window. Afterwards we used the maximal semblance to get the actual value of slowness for every position of the time window.

During the construction of a final migrated image we included amplitude and phase factors (Yilmaz, 2001), which account for the angle dependence of amplitudes (obliquity factor), the spherical spreading, and the wavelet shaping. These extra options allowed us to improve the migrated results.

Application to synthetic data

We applied the velocity-less algorithm to several synthetic 2D data sets. We started from the simplest convolution models: dipping reflection boundary and a syncline model with velocities common for sediments. Then we tested this migration on a model based on real geological situation with steep boundaries and high velocities, which are normal for hard rock environments. The dataset for this complex model was generated using finite-diference approach in TesseralCS-2D modelling software.

Figure 1 shows the models for the simple examples. Velocity of the upper part for both cases was 3000 m/s. We used zero phase wavelet with 30 Hz dominant frequency and trace-length of 1 second. No noise has been added to these models. There were two hundred receivers and the same number of shots; distance between receivers and between shot positions was 10 m. As noted above, horizontal slownesses were calculated by using the semblance approach. For each point in data sets, local slopes were obtained for source and receiver gathers, respectively. Using these values of horizontal slownesses and the arrival time of each sample the oriented attributes (migration velocity (V), vertical traveltime (t_0) and horizontal coordinates (x_m)) were calculated. The attributes t_0 and x_m define the location of migrated data; each sample was placed to the final image in accordance with these two parameters.

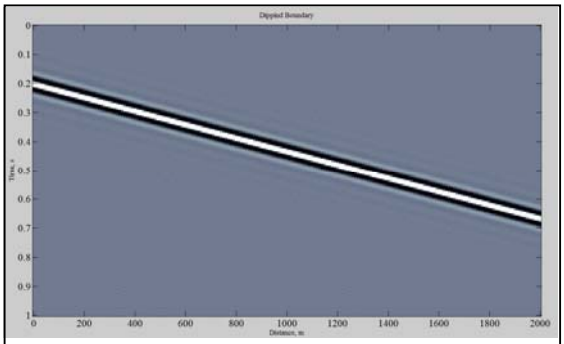

(a) dipping boundary

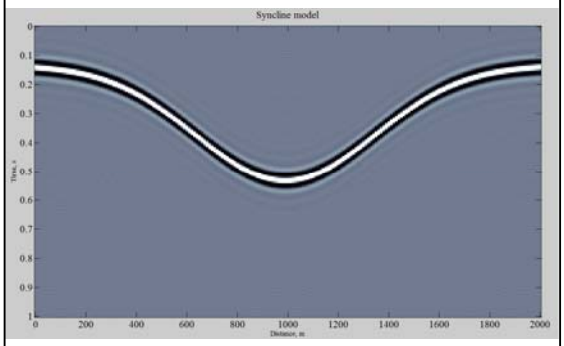

(b) syncline

Figure 1. Convolution models in time scale: (a) dipping boundary, (b) syncline.

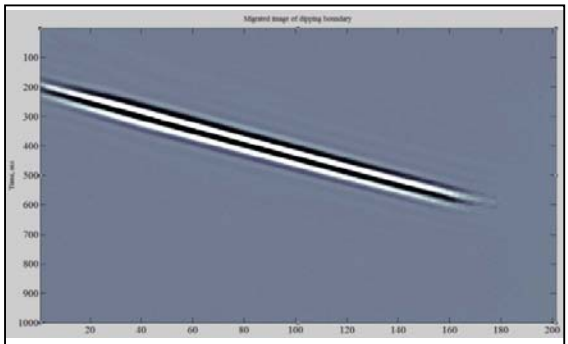

(a) dipping boundary

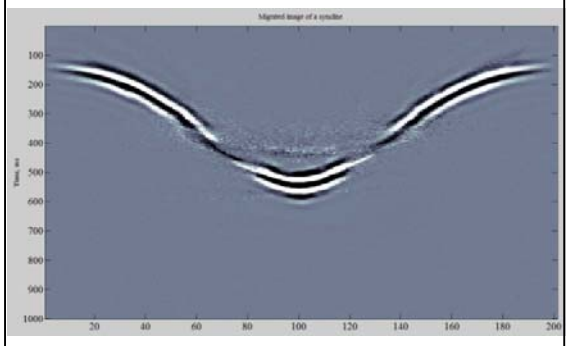

(b) syncline

Figure 2. Migrated images from convolution models: (a) dipping boundary, (b) syncline.

Figure 2 shows migrated images form presented models; the horizontal coordinates correspond to a source-receiver offset. The image from the dipping boundary is imaged clearly, and the slope of the boundary is the same as the slope of the model. On the migrated image of the syncline, both sides of the fold are a slightly blurred. This could be because of insufficient amount of energy which was reflected from these parts of the model. The depth position of the fold and the slopes of its sides are matched with the model.

Next, we tested this velocity-less time migration on a synthetic model which simulates real hard rock geological conditions. Figure 3 shows the velocity model. The values of the velocity and density for each unit are represented in the Table 1. The seismic dataset was obtained using finite-difference method in TesseralCS-2D modelling software. Distance between receivers was 5 m, shots were located at the same positions as the receivers. The Ricker wavelet with a central frequency 80 Hz was chosen for the modelling.

	Rock Unit	**Vp (*m/s*)**	**Density (*kg/m*^{3})**
A	Regolith	2200	2000
B	Volcaniclastic	5500	2800
C	Mafic intrusion	6200	3500
D	Banded Iron Formation	6200	2750
E	Dolerite	6400	2900
F	Felsic Porphyry	6700	3100
G	Fault	5800	2650
H	Shear Zone	5000	2600

Table 1. Description of the 2D model.

Figure 4 shows the migrated image from the hard rock synthetic model. We included the obliquity factor and took into account decay of amplitude with distance and phase factor for each seismic sample. The boundary between regolith and volcaniclastic rocks is displayed very clear. The top of

the mafic intrusion (circled in red) could be distinguished easily; the steep sides of this intrusion are not visible, because most of the energy reflected out of the receivers' locations. The whole felsic porphyry body is also distinctly observed (circled in blue in the figure).

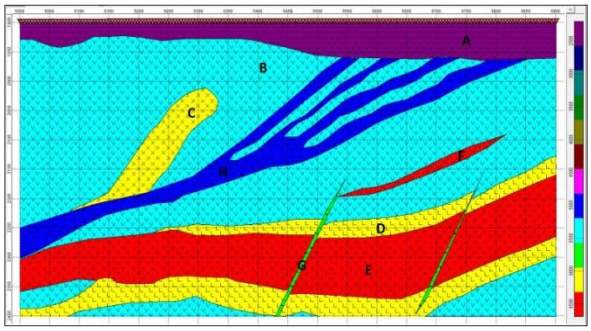

Figure 3. 2D velocity model used to generate

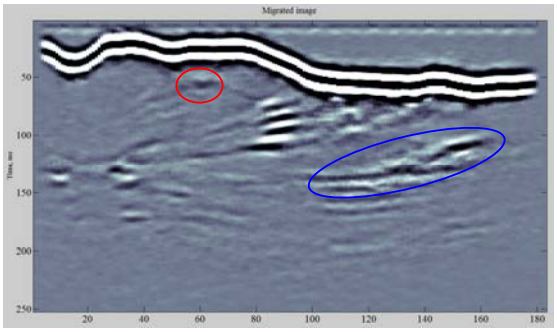

Figure 4. Migration image from the 2D hard

Conclusions

We presented an application of a velocity-less time migration that uses horizontal slownesses in the source and receiver gathers. These local event slopes allowed us to calculate migration velocities, vertical traveltime and horizontal coordinates of the migrated locations for each input sample of the prestack data. We used these attributes to directly map the events into the time-migrated image. We used semblance approach to obtain the local slopes. At the end, we applied amplitude-phase factors before the final summation to improve a quality of the images. This approach was successfully tested on simple convolution models. Finally, we applied the algorithm to construct images from the hard rock model without knowledge of the velocities. This is an important result especially for hard rock sites where the information about velocities is often incomplete. However, this velocity-independent migration should be tested on real data. As part of our future research, we will modify the method to accommodate VSP geometry, explore possibility of using the obtained velocity model as an input for standard migrations.

Acknowledgments

We would like to thank CRC DET consortium for supporting of this research. Also, we would like to thank Andrew Greenwood for the hard rock model.

References

Bóna, A., 2009, Velocityless migration of source gathers: 79th Annual International Meeting, SEG, Expanded Abstracts, 3000-3004.
Cooke, D., Bóna, A., Hansen, B., 2009, Simultaneous time imaging, velocity estimation, and multiple suppression using local event slopes: Geophysics, 74, WCA65–WCA73.
Fomel, S., 2002, Applications of plane-wave destruction filters: Geophysics, 67, 1946–1960.
Fomel, S., 2007, Velocity-independent time-domain seismic imaging using local event slopes: Geophysics, 72, no. 3, S139–S147.
Ottolini, R., 1983a, Signal/noise separation in dip space: Stanford Exploration Project, 37, 143–149.
Ottolini, R., 1983b, Velocity independent seismic imaging: Stanford Exploration Project, 37, 59–68.
Riabinkin, L. A., 1957, Fundamentals of resolving power of controlled directional reception (CDR) of seismic waves, *in* L. Lu, ed., Slant-stack processing, 1991, Society of Exploration Geophysicist, 36–60. (Translated and paraphrased from Prikladnaya Geofizika, 16, 3–36).
Rieber, F., 1936, A new reflection system with controlled directional sensitivity: Geophysics, 1, 97–106.
Schliecher, J., Costa, J.C., Santos, L.T., Novais, A., Tygel, M., 2009, On the estimation of local slopes: Geophysics, 74, no. 4, P25–P33.
Yilmaz, O., 2001, Seismic data processing, 2nd ed.: Society of Exploration Geophysicist.